THE JOURNAL OF COMPARATIVE NEUROLOGY 408:515–531 (1999)

Glycine Immunoreactivity of Multipolar Neurons in the Ventral Cochlear Nucleus Which Project to the Dorsal Cochlear Nucleus

JOHN R. DOUCET,* ADAM T. ROSS, M. BOYD GILLESPIE, AND DAVID K. RYUGO
Center for Hearing Sciences, Departments of Otolaryngology-Head and Neck Surgery and Neuroscience, Johns Hopkins University School of Medicine, Baltimore, Maryland 21205

ABSTRACT

Certain distinct populations of neurons in the dorsal cochlear nucleus are inhibited by a neural source that is responsive to a wide range of acoustic frequencies. In this study, we examined the glycine immunoreactivity of two types of ventral cochlear nucleus neurons (planar and radiate) in the rat which project to the dorsal cochlear nucleus (DCN) and thus, might be responsible for this inhibition. Previously, we proposed that planar neurons provided a tonotopic and narrowly tuned input to the DCN, whereas radiate neurons provided a broadly tuned input and thus, were strong candidates as the source of broadband inhibition (Doucet and Ryugo [1997] J. Comp. Neurol. 385:245–264). We tested this idea by combining retrograde labeling and glycine immunohistochemical protocols. Planar and radiate neurons were first retrogradely labeled by injecting biotinylated dextran amine into a restricted region of the dorsal cochlear nucleus. The labeled cells were visualized using streptavidin conjugated to indocarbocyanine (Cy3), a fluorescent marker. Sections that contained planar or radiate neurons were then processed for glycine immunocytochemistry using diaminobenzidine as the chromogen. Immunostaining of planar neurons was light, comparable to that of excitatory neurons (pyramidal neurons in the DCN), whereas immunostaining of radiate neurons was dark, comparable to that of glycinergic neurons (cartwheel cells in the dorsal cochlear nucleus and principal cells in the medial nucleus of the trapezoid body). These results are consistent with the hypothesis that radiate neurons in the ventral cochlear nucleus subserve the wideband inhibition observed in the dorsal cochlear nucleus. J. Comp. Neurol. 408:515–531, 1999. © 1999 Wiley-Liss, Inc.

Indexing terms: auditory system; biotinylated dextran amine; hearing; inhibition

Auditory nerve fibers innervate the cochlear nucleus in a highly organized and frequency-specific manner referred to as tonotopy (Fekete et al., 1984; Liberman, 1991, 1993; Ryugo and May, 1993). The tonotopic innervation of the anterior ventral cochlear nucleus (AVCN), posterior ventral cochlear nucleus (PVCN), and dorsal cochlear nucleus (DCN) results in all three subdivisions being arranged into a series of isofrequency sheets (Rose et al., 1960; Bourk et al., 1981; Spirou et al., 1993). This organization is also characteristic of most local circuits in the cochlear nucleus, where connections within and between the subdivisions are confined primarily to corresponding isofrequency sheets. However, a few studies have suggested that connections between different isofrequency sheets may exist (Wickesberg and Oertel, 1988; Snyder and Leake, 1988). Recently, we found that certain classes of neurons in the ventral cochlear nucleus (VCN) projecting to a DCN isofrequency sheet reside far outside the corresponding VCN isofrequency sheet (Doucet and Ryugo, 1997). An "off-frequency" projection from the VCN to the DCN is important because it could explain why certain populations of DCN neurons are inhibited by acoustic energy far outside their excitatory tuning curves (e.g., Nelken and Young, 1994). This response property of DCN neurons suggests that the "off-frequency" input from the VCN is inhibitory,

Grant sponsor: National Institute on Deafness and Other Communication Disorders, National Institutes of Health Research; Grant numbers: R01 DC00232, P60 DC00979.

*Correspondence to: Dr. John R. Doucet, Center for Hearing Sciences, Johns Hopkins University School of Medicine, 720 Rutland Avenue, Baltimore, MD 21205. Email: jdoucet@bme.jhu.edu

Received 6 August 1997; Revised 13 January 1999; Accepted 18 January 1999

© 1999 WILEY-LISS, INC.

and we tested this idea by examining the glycine immunoreactivity of VCN neurons that project to the DCN.

Neural circuits intrinsic to the DCN shape the physiological responses to sound of the resident neurons (e.g., Voigt and Young, 1980; Young et al., 1988). These local circuits, however, do not account for all of the response properties of DCN neurons. For example, type II units of the DCN are relatively unresponsive to broadband stimuli even when the stimuli contain energy within the excitatory response area of the neuron (Young and Brownell, 1976). This property implies that type II units within a given isofrequency sheet are inhibited by a source that receives auditory nerve input from other isofrequency sheets (Young et al., 1988). Because this inhibitory source is postulated to be tuned to a wide range of acoustic frequencies, it has been referred to as the "wideband inhibitor" (Nelken and Young, 1994). Wideband inhibition in the DCN is probably not mediated by the inhibitory interneurons of the DCN (Osen et al., 1990; Kolston et al., 1992) because their axons arborize primarily within their respective isofrequency sheet (Lorente de Nó, 1981; Oertel and Wu, 1989; Berrebi and Mugnaini, 1990; Manis et al., 1994).

The source of wideband inhibition might reside in the VCN, because the DCN receives a robust projection from VCN multipolar neurons (Lorente de Nó, 1981; Adams, 1983; Snyder and Leake, 1988; Doucet and Ryugo, 1997). An attractive candidate is the physiological class of VCN units referred to as onset-choppers (Rhode and Smith, 1986). Onset-chopper units are broadly tuned (Rhode and Smith, 1986; Winter and Palmer, 1995; Jiang et al., 1996; Palmer et al., 1996) and they appear to send a collateral axon to the DCN (Smith and Rhode, 1989). They have a multipolar/stellate cell morphology and their axon terminals contain pleiomorphic synaptic vesicles (Smith and Rhode, 1989), a synaptic feature usually associated with an inhibitory neurotransmitter (Uchizono, 1965). These structural characteristics were observed after using the difficult procedure of intracellular recording and filling of single onset-chopper units. As a result, very few onset-chopper units have been labeled; furthermore, because the reaction product faded as the collateral axon entered the DCN, the nature of the projections remains unknown.

Recently, we described the projection patterns of two different populations of VCN multipolar neurons that innervate the DCN in the rat (Doucet and Ryugo, 1997). One population was composed of planar neurons, so named because the dendritic arborizations of their constituents were constrained to isofrequency planes. This feature is consistent with the idea that planar neurons are sharply tuned, and because they also project tonotopically to the DCN, they probably convey "on-frequency" input to DCN neurons. The second population was named radiate neurons because the neurons had dendrites that extended across the VCN isofrequency sheets. Neurons with onset-chopper activity also exhibit this dendritic feature (Smith and Rhode, 1989). The broad tuning of onset-chopper units might be related to their dendrites being contacted by auditory nerve fibers spanning a broad range of characteristic frequencies (Rhode and Smith, 1986; Winter and Palmer, 1995). In this context, radiate neurons in the rat may also be broadly tuned, and with their dendritic morphology and projection pattern, emerge as strong candidates for the role of wideband inhibitor.

If radiate neurons are inhibitory, they should contain high concentrations of an inhibitory neurotransmitter such as glycine or gamma aminobutyric acid (GABA). Numerous immunohistochemical studies have described the types of cochlear nucleus neurons immunostained using antibodies directed against glycine and/or GABA. Putative GABAergic neurons of the VCN have small somata and are primarily distributed around the edge of the nucleus (Wenthold et al., 1986; Osen et al., 1990; Kolston et al., 1992; Moore et al., 1996). Because radiate neurons are large and found within the core of the VCN, they are unlikely to be GABAergic. On the other hand, there are large neurons scattered within the core of the VCN, which are found to be darkly immunostained by using glycine antibodies (Wenthold et al., 1987; Peyret et al., 1987; Aoki et al., 1988; Osen et al., 1990; Kolston et al., 1992). For the present study, our goal was to use a combined retrograde labeling and immunohistochemical protocol in order to test the hypothesis that radiate neurons projecting to the DCN are also enriched with glycine.

MATERIALS AND METHODS

Surgical preparation

The present report is based on data from five male Sprague-Dawley rats weighing between 250 and 400 g. All animals and procedures were used in accordance with the NIH guidelines and the approval of the Johns Hopkins Medical School Animal Care and Use Committee. Each rat was anesthetized with an intraperitoneal injection of sodium pentobarbital (40 mg/kg) and given an intramuscular injection of atropine sulfate (0.05 mg). When the animal was areflexic to a paw pinch, the soft tissues overlying the dorsal aspect of the skull were cut and reflected, and an opening on one side of the occipital bone was drilled to expose the posterior aspect of the cerebellar cortex. A portion of the cerebellum extending from the vermis towards the flocculus was aspirated so that the entire DCN could be clearly viewed. An electrode (inside tip diameter, 20–30µm) filled with a 10% (w/v) solution of biotinylated dextran amine (BDA, mw 10,000, Molecular Probes; Eugene, OR) in 0.01 M phosphate buffer (pH 7.4) was then advanced with a hydraulic microdrive to a depth of 250µm below the DCN surface. The application of positive current pulses (5µA, 7 seconds on, and 50% duty cycle) for 5 minutes was used to inject the BDA solution. Afterwards, the incision was closed and the animal was allowed to recover.

Tissue processing

Approximately 24 hours after the injection, animals were administered a lethal dose of sodium pentobarbital. When the animal was areflexic to a paw pinch, it was transcardially perfused with 25 ml of a fixative solution of 0.1 M phosphate-buffered saline (pH 7.4) with 1% sodium nitrite (a vasodilator) followed immediately by 250 ml of a solution of 0.1 M phosphate buffer containing 4% paraformaldehyde and 0.5% glutaraldehyde (pH 7.4). The brainstem was then dissected from the skull, postfixed in the fixative solution for 90 minutes at 21°C, and sectioned in the coronal plane (50µm thickness) using a Vibratome. Sections were serially collected in 0.05 M Tris buffer (TB), pH 7.5, containing 0.85% sodium metabisulfite, treated for 10 minutes at 21°C in TB containing 0.1 M sodium borohydride, and washed with TB. Sections were then incubated for 90 minutes at 21°C in TB with the addition of

10% normal goat serum (NGS) to block nonspecific binding sites, and placed overnight (4°C) in TB containing the rabbit anti-glycine antibody (1:1,200, Chemicon; Temecula, CA) and 1% NGS. In some instances, we added 0.1% Triton X-100 to the primary antibody solution, but because we could not detect an improvement in staining, this step was not always included. The Chemicon antibody to glycine has minimal cross-reactivity with other amino acids as verified in the retina (Kalloniatis and Fletcher, 1993) and in the superior olivary complex (Spirou and Berrebi, 1997). No immunoreactivity was ever observed in control sections where the primary antibody was omitted from the protocol (see Fig. 4), or where the primary antibody was preadsorbed with antigen (a glycine-glutaraldehyde-bovine serum albumin (BSA) complex kindly provided by Dr. Robert Wenthold).

The next day, sections were washed with a solution of 0.05 M Tris buffer, pH 7.5, containing 0.85% NaCl (TBS). In order to inactivate any peroxidase already present in the tissue, sections were incubated for 15 minutes (21°C) in a solution of 0.3% hydrogen peroxide in 0.1 M phosphate-buffered saline (pH 7.4). Sections were then washed again with TBS and incubated for 3 hours (21°C) in TBS containing streptavidin conjugated to indocarbocyanine (Cy3; 1:10,000, Jackson ImmunoResearch Laboratories; West Grove, PA), peroxidase-conjugated goat anti-rabbit antibodies (Jackson ImmunoResearch Laboratories, 1:200), and 1% NGS. Lastly, the sections were washed in TBS, mounted on slides, air-dried for 15–30 minutes, and coverslipped with Vectashield mounting medium (Vector Laboratories; Burlingame, CA). At this point, neurons filled with the BDA-streptavidin-Cy3 complex appeared red when viewed under a fluorescent microscope with a rhodamine barrier filter (see Fig 2).

Data collection

We focused our analysis on retrogradely labeled planar and radiate neurons within the magnocellular core of the VCN. Other types of VCN neurons that project to the DCN (e.g., microneurons of the granule cell domain) were not examined in this study. Each section through the VCN was viewed using a fluorescent microscope and a collection of retrogradely labeled planar and radiate neurons were mapped and photographed. We limited our analysis to neurons located near the surface of the tissue section because the glycine immunostaining was restricted to these regions due to the failure of the antibodies and reagents to diffuse more than 10μm into the tissue. We used thick sections rather than thin sections because with small injection sites, only 5–8 radiate cells were labeled in each experiment. Since we could not predict where these radiate neurons would be located, protocols employing thinner tissue sections were impractical because they would have resulted in too many sections to be handled efficiently.

In each animal, one to two radiate neurons and 10–15 planar neurons were mapped and photographed. We analyzed only a subset of the planar neurons near the tissue surface because the quality of glycine immunostaining decreased with time spent on classification, mapping, and photographing. The sections containing the photographed neurons were removed from the slides, washed with TBS, and then incubated for 10 minutes (21°C) in 0.05 M Tris buffer (pH 7.5) containing 0.004% diaminobenzidine (DAB) and 0.05% hydrogen peroxide. This last step completed the immunocytochemical protocol and immunoreactive cells appeared brown in color when viewed with brightfield microscopy. After washing the sections with TBS, they were remounted on slides and coverslipped with Vectashield. The previously photographed cells were identified using fluorescent landmarks and blood vessels (see Figs. 5–8), the microscope was switched to brightfield illumination, and glycine immunostaining was viewed in the same focal plane as that of the retrogradely labeled cell.

The double-labeling protocol described above was chosen after evaluating alternative approaches. A double-labeling method calling for granular reaction product (DAB) from retrograde transport and diffuse black reaction product (metal-intensified DAB) from immunocytochemical processing was rejected because of the difficulty in differentiating dark brown from light black. Double labeling protocols that utilized separate fluorescent markers were abandoned because of the autofluorescence produced by glutaraldehyde in the fixative. Glutaraldehyde was a necessary component of the fixative because the Chemicon antibody only recognized glycine cross-linked to proteins by glutaraldehyde. The background fluorescence, combined with variable glycine immunostaining in cochlear nucleus neurons (see Results), made identification of labeled neurons difficult. Fortunately, the background fluorescence produced by glutaraldehyde was low enough to enable visualization of BDA-filled neurons using streptavidin conjugated to Cy3. Because protocols combining fluorescent and brightfield chromophores have been used successfully for the simultaneous detection of two antigens within cells (Albanese and Bentivoglio, 1982; Eckenstein and Sofroniew, 1983), we applied this strategy in this study.

All photographs were collected using a cooled-CCD color camera (Hamamatsu C5810), digitized, and altered (if necessary) using procedures consistent with standard darkroom techniques (Adobe Photoshop 3.0). Final images were printed in high-resolution format with a color printer (Fuji Pictrography 3000).

Optical density measurements

The glycine immunoreactivity of cochlear nucleus neurons was graded from light to dark. In order to evaluate the immunoreactivity of planar and radiate cells, we compared the intensity of their immunostaining with a population of known excitatory neurons (pyramidal cells of the DCN) and with two populations of known glycinergic neurons (cartwheel cells of the DCN and principal cells of the medial nucleus of the trapezoid body (MNTB). To quantify these comparisons, cells of each class were viewed at high magnification (×63 oil immersion objective) using brightfield microscopy. A gray scale image of each cell was then captured using a CCD camera while holding all image-gathering parameters constant. The cell body was outlined and the optical density was determined for each cell (Adobe Photoshop 3.0).

Criteria for data presentation

The five experiments described in this paper were selected from a larger pool of animals that received injections of BDA in the DCN. Our selection criterion was based solely on whether or not the BDA injection site spread into the intermediate or dorsal acoustic stria. When

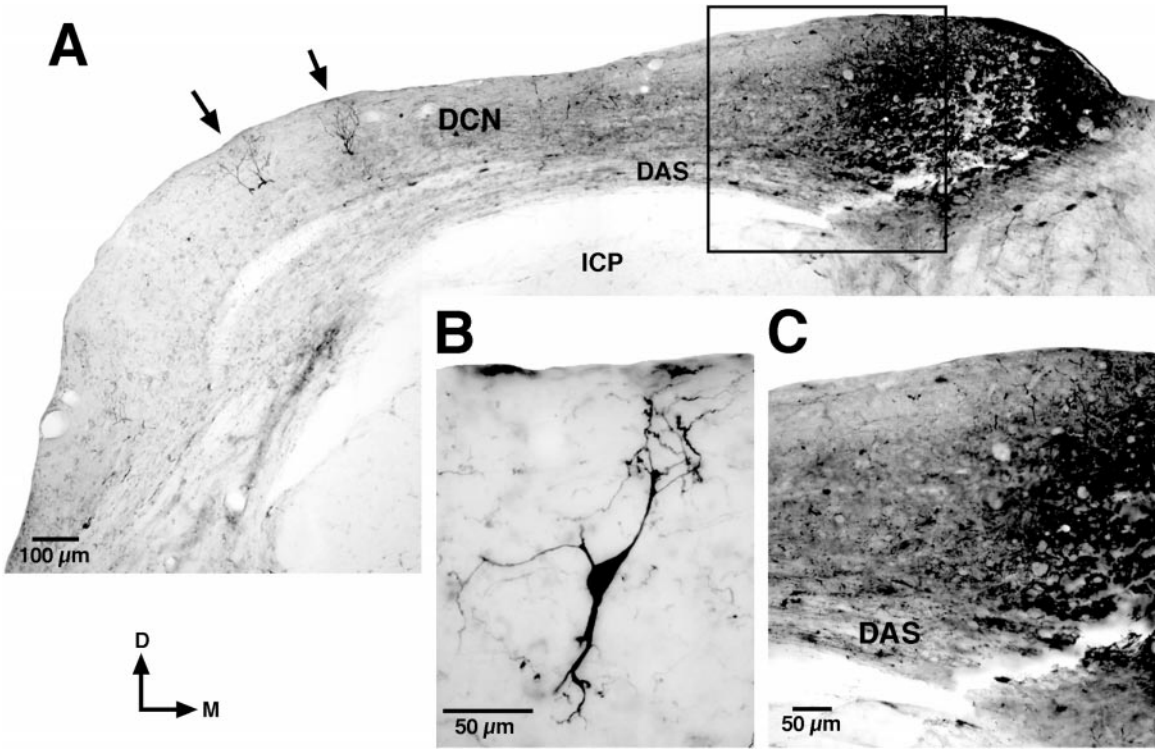

Fig. 1. Typical dorsal cochlear nucleus (DCN) labeling when the biotinylated dextran amine (BDA) injection site involves the underlying dorsal acoustic stria (DAS). **A:** Coronal section showing the black BDA reaction product of the injection site in the dorsomedial pole of the DCN, where the injection appears to have damaged the axons of the DAS. The boxed area in A is shown at higher magnification in C. When there is contamination by axons-of-passage within the DAS, pyramidal and giant cells located lateral to the injection site are labeled. The apical dendrites (arrows) of two pyramidal cells are evident. **B:** Higher magnification of a labeled pyramidal cell found in another section of the DCN. D, dorsal; ICP, inferior cerebellar peduncle; M, medial.

the injection site infringed upon either of these dorsal output tracts, pyramidal and giant cells of the DCN along with octopus cells of the VCN were labeled (Fig. 1). To reduce errors due to "fibers-of-passage," we included cases only in which the injection site was confined to the DCN. Thus, we infer that axon terminals arising from cells of the VCN took up BDA in the DCN, and then transported the BDA back to the cell body.

RESULTS

Retrograde labeling and cell classification

In each experiment, the BDA injection site was located just below the DCN surface, approximately midway along its dorsomedial-ventrolateral axis. Isofrequency sheets are organized in the DCN along its long axis, where low frequency sheets are found in the ventrolateral region and progressively higher frequency sheets are stacked toward the dorsomedial tip (Rose et al., 1960; Ryugo et al., 1981; Kaltenbach and Lazor, 1991; Ryugo and May, 1993). A typical injection site is displayed (Fig. 2A,B; also Figs. 5 and 6). In all five experiments, the reaction product from each injection site was localized to a narrow band in the DCN and did not encroach upon the underlying acoustic striae (compare Fig. 2B and Fig. 1C). Our methods were nearly identical to those described in a previous study (Doucet and Ryugo, 1997), with the major difference being the use of streptavidin conjugated to Cy3 rather than DAB to visualize labeled neurons. As a result, cells and associated structures that were filled with BDA fluoresced bright red (Fig. 2).

In the VCN, there was a thin, red stripe of fluorescent label that ran across the medial-to-lateral axis of the nucleus (Fig. 2C). The thickness (50–150μm), orientation, and three-dimensional organization of the fluorescent

Fig. 2. Focal injection of biotinylated dextran amine (BDA) into the dorsal cochlear nucleus (DCN) and retrograde labeling observed in the ventral cochlear neucleus (VCN). In this experiment, BDA labeling was visualized using streptavidin conjugated to indocarbocyanine (Cy3), a molecule that fluoresces red. **A:** Coronal section through the DCN displaying a BDA injection site centered in the middle of the DCN. Retrogradely labeled cells of the granule cell domain are seen ventrolaterally, at the border between the DCN and VCN. **B:** Magnified view of the injection site. Notice that the injection is confined to the DCN and the axons of the underlying dorsal acoustic stria (DAS) are not involved. Furthermore, no pyramidal or giant cells were observed in this DCN. **C:** Coronal section through the VCN at the level of the auditory nerve root (AN). There are labeled cells in the peripheral shell of the nucleus and in the core of the VCN. The retrograde labeling in the core is dominated by a fluorescent stripe composed of cells (green and white arrowheads), their dendrites, and axons from various sources. A few large retrogradely filled cells (e.g., yellow arrowhead) are found outside the stripe and are known as radiate neurons. **D:** Magnified view of the radiate neuron. **E:** Magnified view of cells located inside the fluorescent stripe. The smaller somata represent planar neurons (green arrowheads) and the large cell is probably a radiate neuron (white arrowhead). See text for details of classification procedure. D, dorsal; ICP, inferior cerebellar peduncle; M, medial.

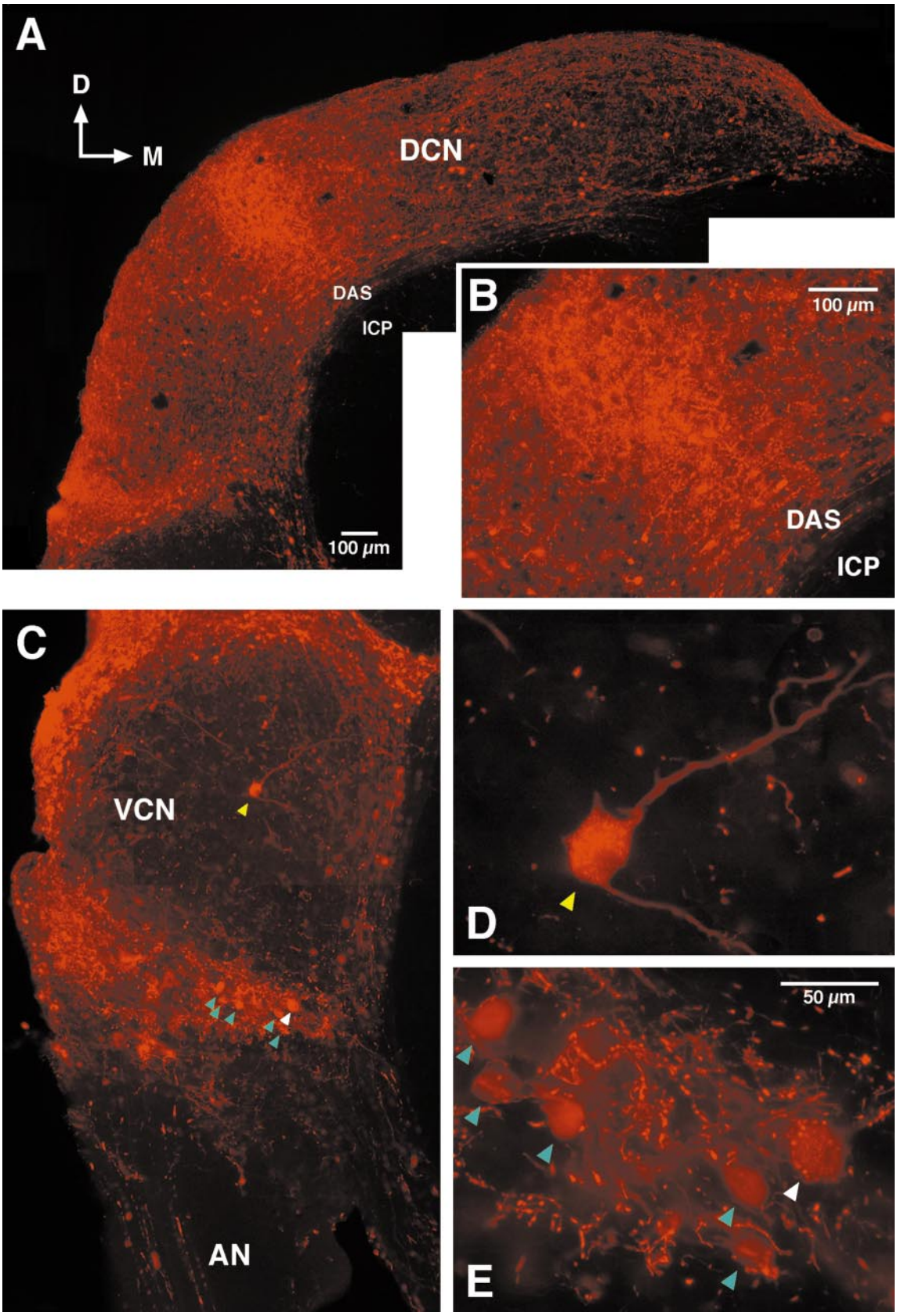

Figure 2

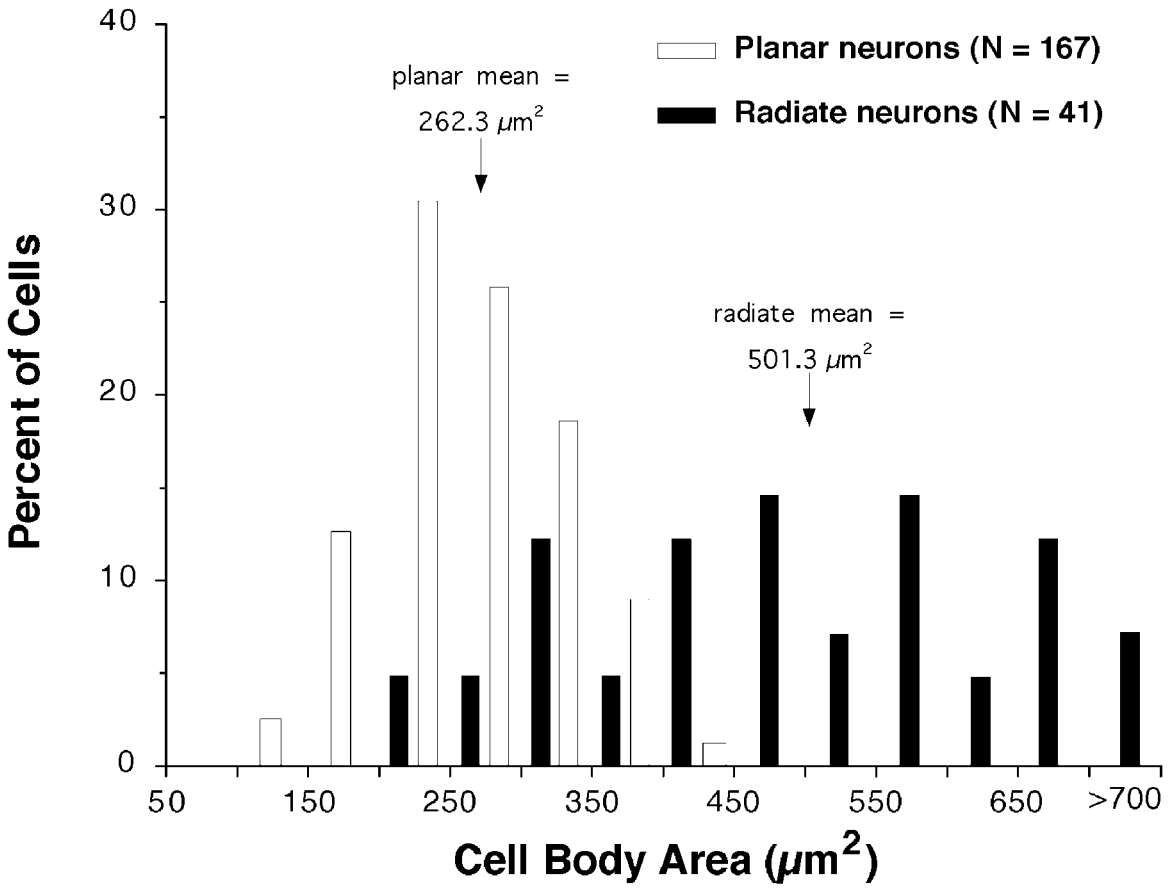

Fig. 3. Distribution of cell body silhouette areas for radiate and planar neurons. The cells used to form this histogram were taken from another study (Doucet and Ryugo, 1997) where the dendrites of the retrogradely labeled cells were reconstructed sufficiently to allow placement of the neurons into the two classes. Although the two distributions overlap, notice that planar neurons are never as large as the largest radiate neurons, and that few radiate neurons are smaller than the mean cell body area for the planar distribution. These size properties were used to help identify retrogradely labeled ventral cochlear nucleus (VCN) neurons.

stripe resemble a typical isofrequency sheet where labeled cell bodies, axons, and terminals are mostly found (Fig. 2C). This result reveals that the bulk of the connections between the DCN and VCN are between corresponding isofrequency sheets. In the regions of the VCN flanking the auditory nerve root, occasional large BDA-filled neurons can be found outside the labeled stripe (Fig. 2C). The large somatic size and radiating dendritic trajectory of such neurons differ markedly from those of neurons inside the stripe, and they match the descriptions of radiate neurons (Doucet and Ryugo, 1997). Radiate neurons can also be found inside the labeled stripe (Fig. 3B of Doucet and Ryugo, 1997), but such cases are rare. Labeled neurons within the stripe typically have dendrites that are confined to the plane defined by the stripe, and they fit the descriptive criteria for planar neurons. In addition to their dendritic orientations, another distinguishing feature between the two classes is cell body size (e.g., compare the radiate neuron in Fig. 2D with planar neurons [green arrowheads] in Fig. 2E). On average, the somata of radiate neurons (silhouette area, 501.3 ± 168.3μm^2) are much larger than those of planar neurons (silhouette area, 262.3 ± 62.7μm^2). The distribution of cell body size for the two classes of neurons is illustrated (Fig. 3). Although the two distributions overlap, the somata of radiate neurons reach sizes that are never observed for planar neurons, whereas radiate neurons are seldom smaller than the mean size of planar neurons. Analysis of the relative numbers of labeled neurons revealed that labeled planar neurons outnumbered labeled radiate neurons by approximately a factor of eight (Doucet and Ryugo, 1997).

Our goal was to determine any difference in glycine immunoreactivity between planar and radiate neurons. This objective required us first to classify the retrogradely labeled VCN neurons into one of these two cell groups and then to immunostain the tissue for glycine. Due to time limits imposed by our experimental protocol (see Materials and Methods), we chose to analyze the immunostaining of only the most obvious examples of radiate and planar neurons. Radiate neurons were outside the stripe, had at least one dendrite oriented in a dorsal-ventral direction, and had a cell body at least two standard deviations larger than the mean cell body size of cells inside the stripe. Our sample of planar neurons was located inside the stripe, and each had a cell body whose size was below the average for all cells inside the stripe. In other words, we selected only the smallest labeled cells within the stripe. We identified and analyzed at least ten planar neurons from

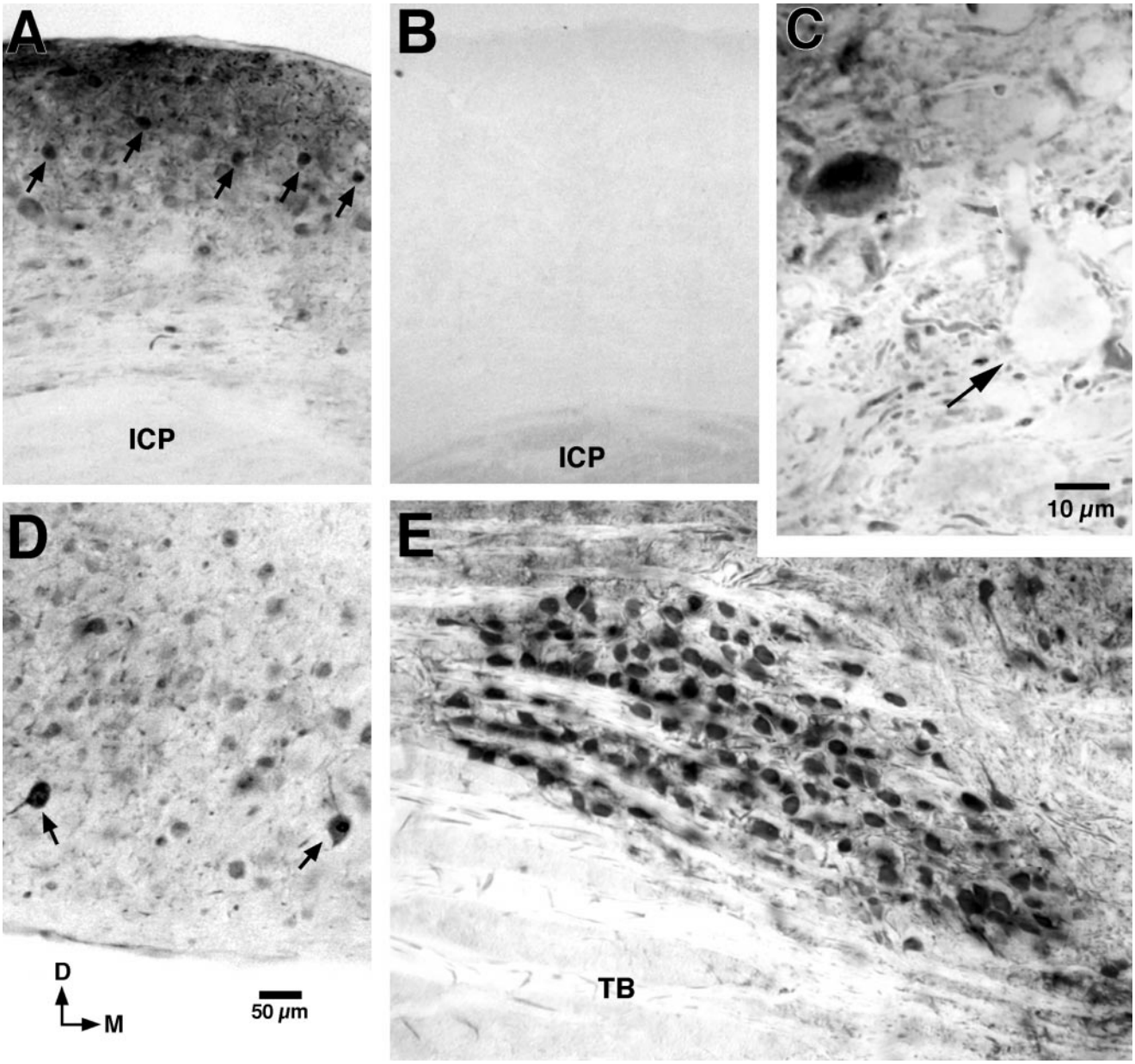

Fig. 4. Glycine immunoreactivity observed in the cochlear nucleus and medial nucleus of the trapezoid body (MNTB). **A:** Coronal section through the dorsal cochlear nucleus (DCN) illustrates the immunostaining observable in all layers, and it is most intense in the superficial layers. Many cells are immunostained to some degree, and the most darkly labeled neurons (arrows) are presumably cartwheel cells located near the pial surface. **B:** The adjacent DCN section served as a control, in which the primary antibody was omitted from the immunoprocessing procedure. There is no staining. Primary antibody omission or antibody preadsorption yielded identical results. **C:** High magnification micrograph of unlabeled DCN pyramidal cell (arrow) and a darkly immunostained cartwheel cell. Pial surface is towards the top of the panel. **D:** A section through the anteroventral cochlear nucleus (AVCN) illustrates two large and darkly stained neurons (arrows). **E:** A section through the MNTB shows the intense immunoreactivity of the neurons within this nucleus. Whereas DCN pyramidal cells served as the standard for glycine-immunonegative neurons, MNTB principal cells and DCN cartwheel cells served as the standards for glycine-immunopositive neurons. Scale bar in D applies to A, B, and E. D, dorsal; ICP, inferior cerebellar peduncle; M, medial; TB, trapezoid body.

each experiment, whereas the number of radiate neurons ranged from five to eight.

Glycine immunostaining

The pattern of glycine immunoreactivity we observed in the cochlear nucleus and superior olivary complex was consistent with the results of previous studies. There have been published descriptions of glycine immunostaining within the cochlear nucleus in a variety of species, including guinea pigs (Wenthold et al., 1987; Saint Marie et al., 1991; Kolston et al., 1992), rats (Mugnaini, 1985; Peyret et al., 1987; Aoki et al., 1988; Gates et al., 1996), mice

(Wickesberg et al., 1991), cats (Osen et al., 1990), and baboons (Moore et al., 1996). As these studies reported, the majority of the immunostained cells and structures were found in the middle and superficial layers of the DCN (Fig. 4A). In the DCN, the most darkly stained neurons were small to medium-sized cells (presumably cartwheel cells) distributed within 200μm of the pial surface (Fig. 4A, C). DCN pyramidal neurons were occasionally immunostained, but their staining intensity tended to be comparable to background levels (Fig. 4C). In the VCN, the most intense immunoreactivity was found in a handful of large cells scattered throughout the magnocellular core (Fig. 4D) and in smaller cells situated along the border of the nucleus. Sparse labeling was observed in the octopus cell area of the PVCN and in the granule cell domain. Within the superior olivary complex, neurons of the MNTB stood out as some of the most intensely immunoreactive neurons in the brainstem (Fig. 4E). Previous glycine immunocytochemical studies had likewise noted the dark staining of MNTB neurons (Wenthold et. al., 1987; Helfert et al., 1989; Spirou and Berrebi, 1997), consistent with their known glycinergic projection to the lateral superior olive (Moore and Caspary, 1983; Bledsoe et al., 1990). Control sections that were processed with the primary antibody either preadsorbed or deleted had no staining (e.g., Fig. 4B).

Retrogradely labeled radiate neurons exhibited intense glycine immunoreactivity after completion of the immunohistochemical protocol. Typical examples from different experiments are illustrated (Figs. 5 and 6). The top two panels of each figure show sections through the DCN containing the injection site. In both cases, the injection site is confined to the DCN and does not damage the underlying axons in the dorsal output tracts. A neuron in the PCVN is shown (Fig. 5) that exhibits all three features which identify radiate neurons: (1) it is located far outside the stripe of retrograde labeling, (2) its cell body is larger than all neurons found within the labeled stripes throughout the VCN, and (3) one prominent dendrite (arrows in Fig. 5C) runs dorsally, perpendicular to the plane of VCN isofrequency sheets. When the same field is viewed by brightfield illumination in order to examine glycine immunoreactivity, many neurons are observed to be immunostained (Fig. 5D). The retrogradely labeled radiate neuron, however, is clearly the most prominent neuron in the field by virtue of its large somatic size and intensity of staining. An example of an intensely stained radiate cell in the AVCN is illustrated in Figure 6.

Although 5–8 retrogradely labeled VCN neurons were classified as radiate neurons in each rat, only one or two of these were located within regions of the tissue containing immunoreactivity. Consequently, a total of seven radiate neurons were evaluated from the five experiments, and although the population was small, we found that all were darkly immunostained for glycine.

In contrast to radiate neurons, the staining of planar neurons was light and frequently comparable to background levels (Figs. 7 and 8). A typical planar neuron was located within the narrow fluorescent stripe, had a medium-sized cell body, and displayed at least one prominent dendrite that ran within the stripe. The low staining level of planar neurons could not be attributed to incomplete penetration of antibody reagents because we purposely photographed and evaluated planar neurons that were located on the surface of the tissue sections. All planar neurons included in our analysis had darkly stained neurons located nearby and within the same focal plane (asterisks in Figs. 6D and 7D). For each of the five rats, between 10 and 15 planar neurons were photographed and evaluated for the intensity of their immunoreactivity, and all planar neurons were either unstained or lightly stained.

An important characteristic of the glycine immunocytochemistry was that the darkness of staining was distributed along a graded continuum from light to dark (Figs. 4–8). Because large numbers of neurons were variably immunoreactive, it is clear that "glycinergic" neurons were not the only cells stained by the immunohistochemical protocol. This result is consistent with the findings of prior studies but raises an important question with respect to our goals, namely, how do we interpret the immunostaining of planar and radiate neurons in order to draw conclusions about whether or not they are glycinergic?

Glycinergic neurons were distinguishable by the intensity of their immunoreactivity. Glycinergic neurons reportedly contain a 10- to 100-fold higher concentration of glycine than nonglycinergic neurons (Ottersen et al., 1990); thus, glycinergic neurons are expected to be much more darkly stained than other cells. Such a distinction was observed in our data by comparing the immunostaining of DCN cartwheel cells (Fig. 4A, C) and MNTB principal neurons (Fig. 4E) to that of DCN pyramidal cells (Fig. 4C). Cartwheel cells and MNTB principal neurons are glycinergic; thus, their immunostaining should reflect neurotransmitter pools of glycine. In contrast, pyramidal cells are projection neurons that exert excitatory influences in the inferior colliculus (Semple and Aitkin, 1980; Oliver, 1984), and they have been used to characterize immunostaining expected for metabolic pools of glycine (Osen et al., 1990; Kolston et al., 1992; Moore et al., 1996). By comparing the immunostaining of planar and radiate cells with these other cell populations, we sought to infer the role played by glycine in these two classes of VCN neurons.

The immunostaining intensities of radiate and planar neurons along with members of the "reference" cell populations described above were quantified and compared using measurements of optical density. These comparisons were made for three animals where sections through the DCN (n = 3) and superior olive (n = 1) were immunoreacted along with VCN sections containing planar and radiate neurons. The distributions of optical densities for the

Fig. 5. Glycine immunoreactivity observed in a retrogradely labeled radiate neuron in the posterior ventral cochlear nucleus (PVCN). Biotinylated dextran amine (BDA)-labeled structures appear white in the photomicrographs produced using fluorescent microscopy (A– C, and E). **A** and **B:** In this animal, the BDA injection site is illustrated in two sections through the dorsal cochlear nucleus (DCN). Notice that the reaction product is confined to the DCN and does not extend into the underlying dorsal acoustic stria (DAS). **C:** Coronal section through the PVCN containing a retrogradely labeled radiate neuron located outside the labeled isofrequency stripe. Arrowheads highlight a prominent dendrite of this radiate cell running dorsally. Asterisks are adjacent to nearby blood vessels evident in C–F. **D:** Brightfield photomontage of glycine immunostaining in the same field and focal plane viewed in C. Although many PVCN neurons are immunostained, note that the radiate cell is the largest and one of the most darkly immunostained neurons in the field. The bottom two panels display the retrograde labeling (**E**) and the glycine immunoreactivity (**F**) of the radiate neuron at high magnification. Scale bars in left panels apply across respective horizontal rows. ICP, inferior cerebellar peduncle; V, descending tract of the trigeminal nerve.

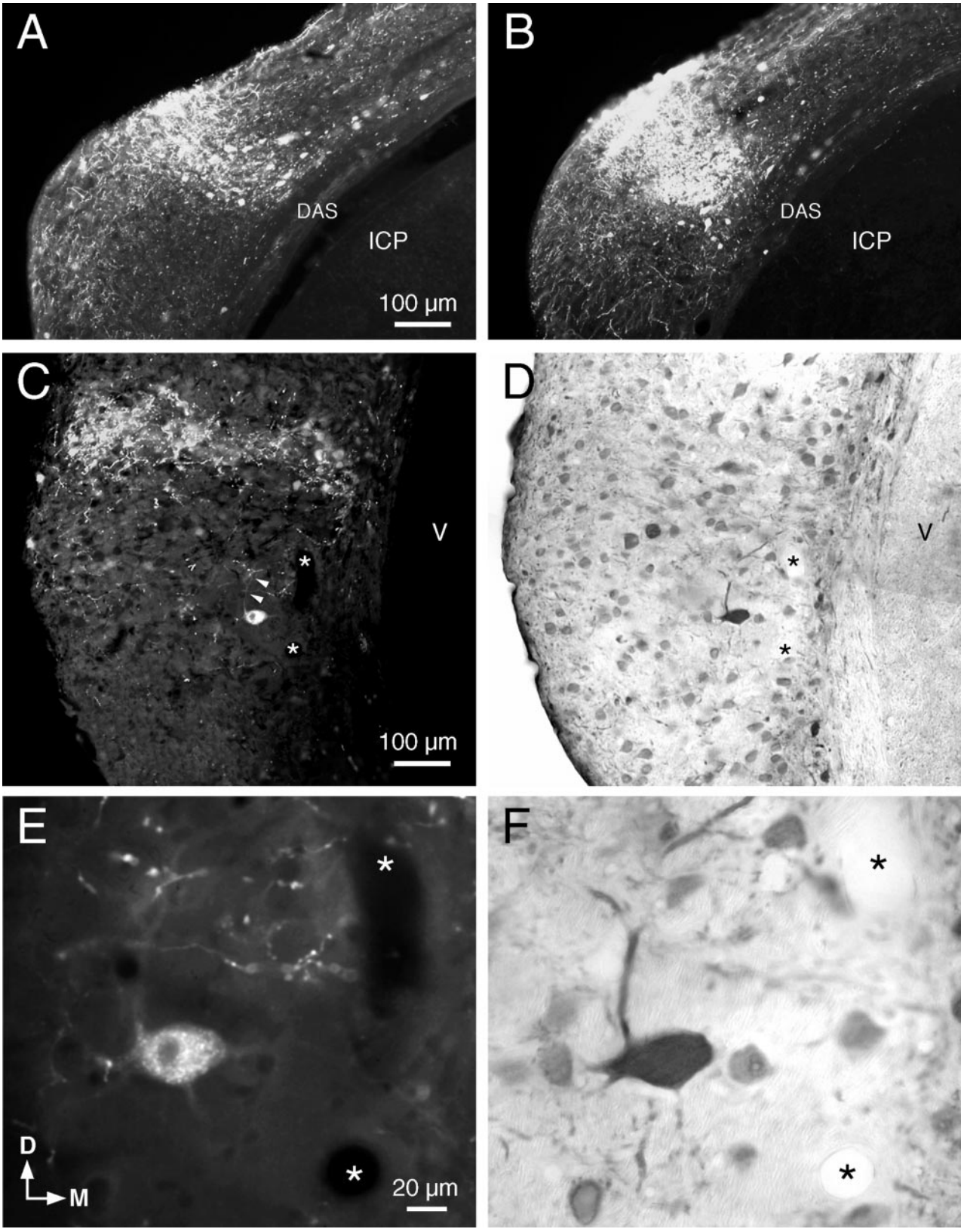

Figure 5

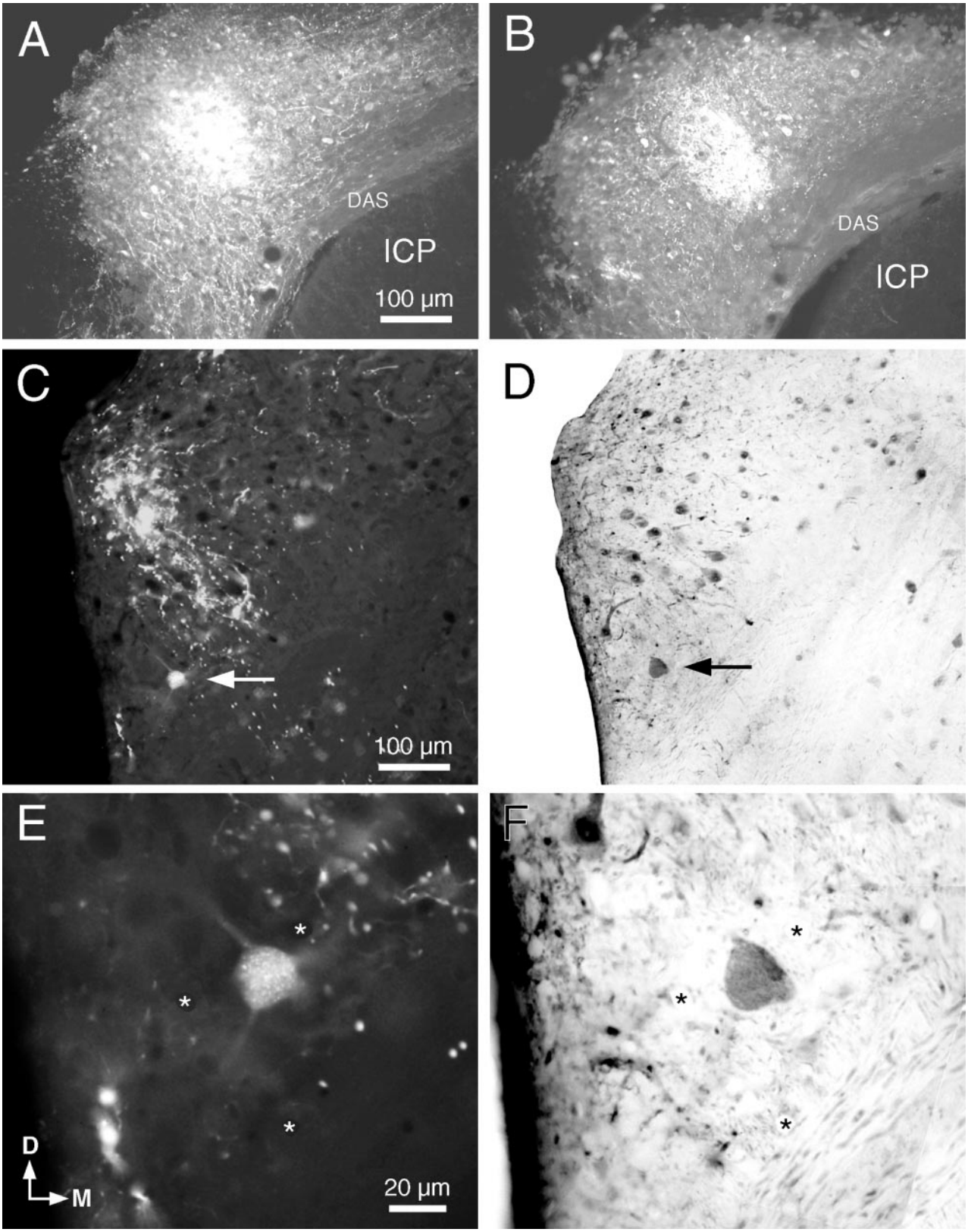

Fig. 6. Glycine immunoreactivity observed in a retrogradely labeled radiate neuron in the anteroventral cochlear nucleus (AVCN). **A** and **B:** Biotinylated dextran amine (BDA) injection site observed in two sections illustrating that the injection site is confined to the dorsal cochlear nucleus (DCN) and does not extend into the underlying dorsal acoustic stria (DAS). **C:** Coronal section through the AVCN showing a retrogradely labeled radiate neuron (arrow) with at least two thick dendrites, with the ventrally directed dendrite extending across isofrequency sheets. **D:** Brightfield photomontage reveals the same field and focal plane following glycine immunostaining. The arrow points to the retrogradely labeled radiate cell which is one of the most darkly immunostained neurons in the field. The bottom two panels display the retrograde labeling (**E**) and the glycine immunoreactivity (**F**) of the radiate neuron at higher magnification. Asterisks denote small blood vessels seen in E and F. Scale bars in left panels apply across respective horizontal rows. ICP, inferior cerebellar peduncle.

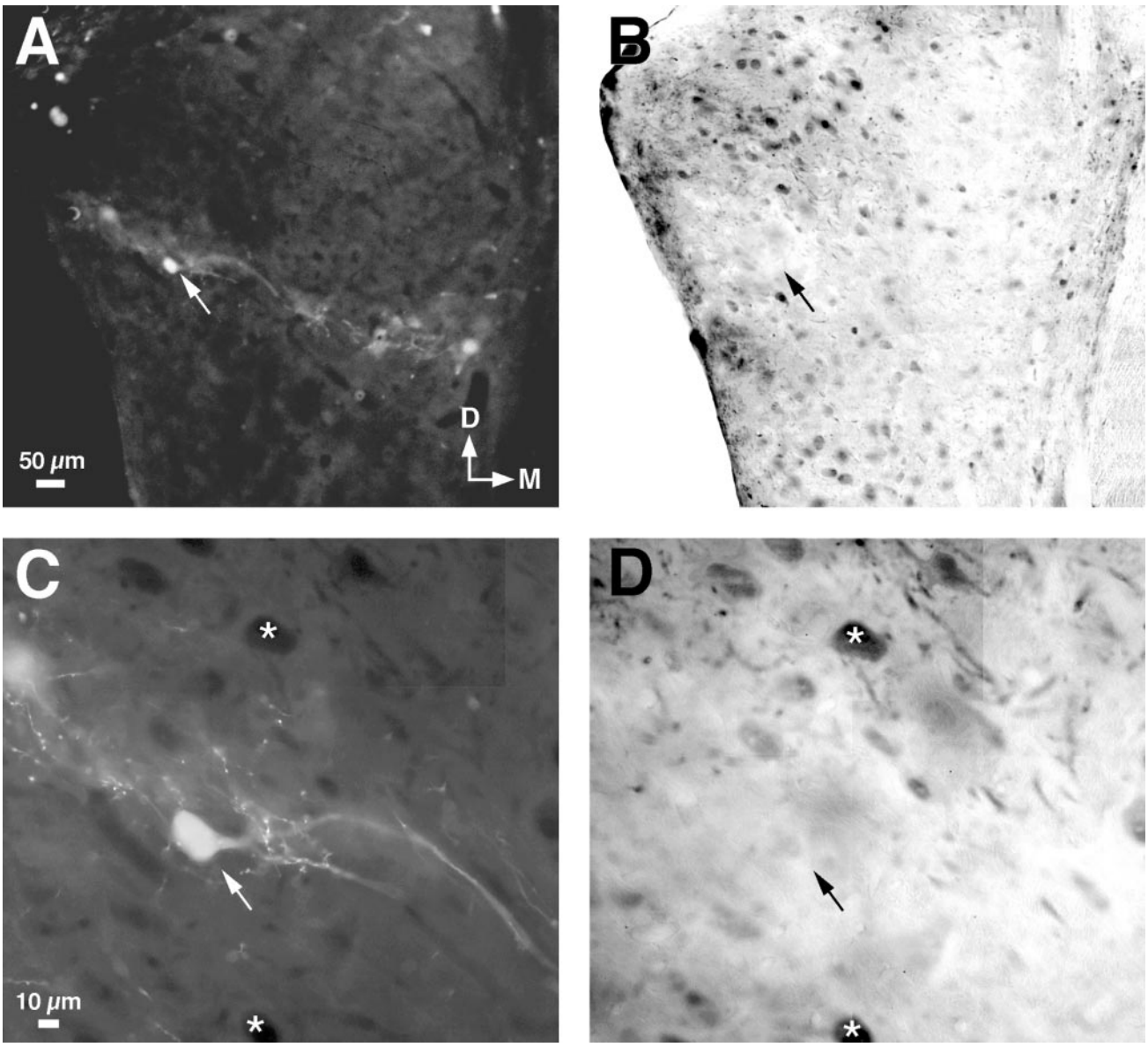

Fig. 7. Retrogradely labeled planar neurons typically do not stain with antibodies directed against glycine. **A:** Fluorescent micrograph of a coronal section through the posterior ventral cochlear nucleus (PVCN) containing several biotinylated dextran amine (BDA)-filled planar neurons within the labeled stripe. A planar neuron (arrow) is readily apparent and one of its dendrites can be followed away from the cell body within the stripe. **B:** Brightfield photomontage of glycine immunostaining in the same field of view and same focal plane as in A. The arrow indicates the spot occupied by the unlabeled planar cell. The retrogradely labeled planar cell (**C**) and its glycine immunonegativity (**D**) are displayed at higher magnification. Asterisks denote two glycine-immunoreactive cells seen in C and D. Even though these two nearby cells are darkly immunostained, the immunoreactivity of the planar neuron (arrow in both C and D) is indistinguishable from background. Scale bars in A and C apply to respective horizontal rows. D, dorsal; M, medial.

neuron populations in three different animals are illustrated, in which a value of 255 represents black and zero signifies white (Fig. 9). Optical density values within each animal were pooled across tissue sections because nearly identical distributions were found for MNTB principal neurons and DCN pyramidal cells collected from different sections. Consistent with the examples of each population shown in Figure 4, the average staining intensity observed for DCN cartwheel cells and MNTB principal neurons (glycinergic cells) was significantly greater than for DCN pyramidal cells (nonglycinergic cells). Likewise, radiate neurons were always more darkly stained than any member of the class of planar neurons. Most importantly, the immunostaining of radiate neurons was comparable to that seen for cartwheel cells and MNTB principal neurons, whereas the range of immunoreactivity observed for planar cells overlapped with that of DCN pyramidal cells.

DISCUSSION

The central finding of this study is that two distinct populations of multipolar neurons, each of which project to

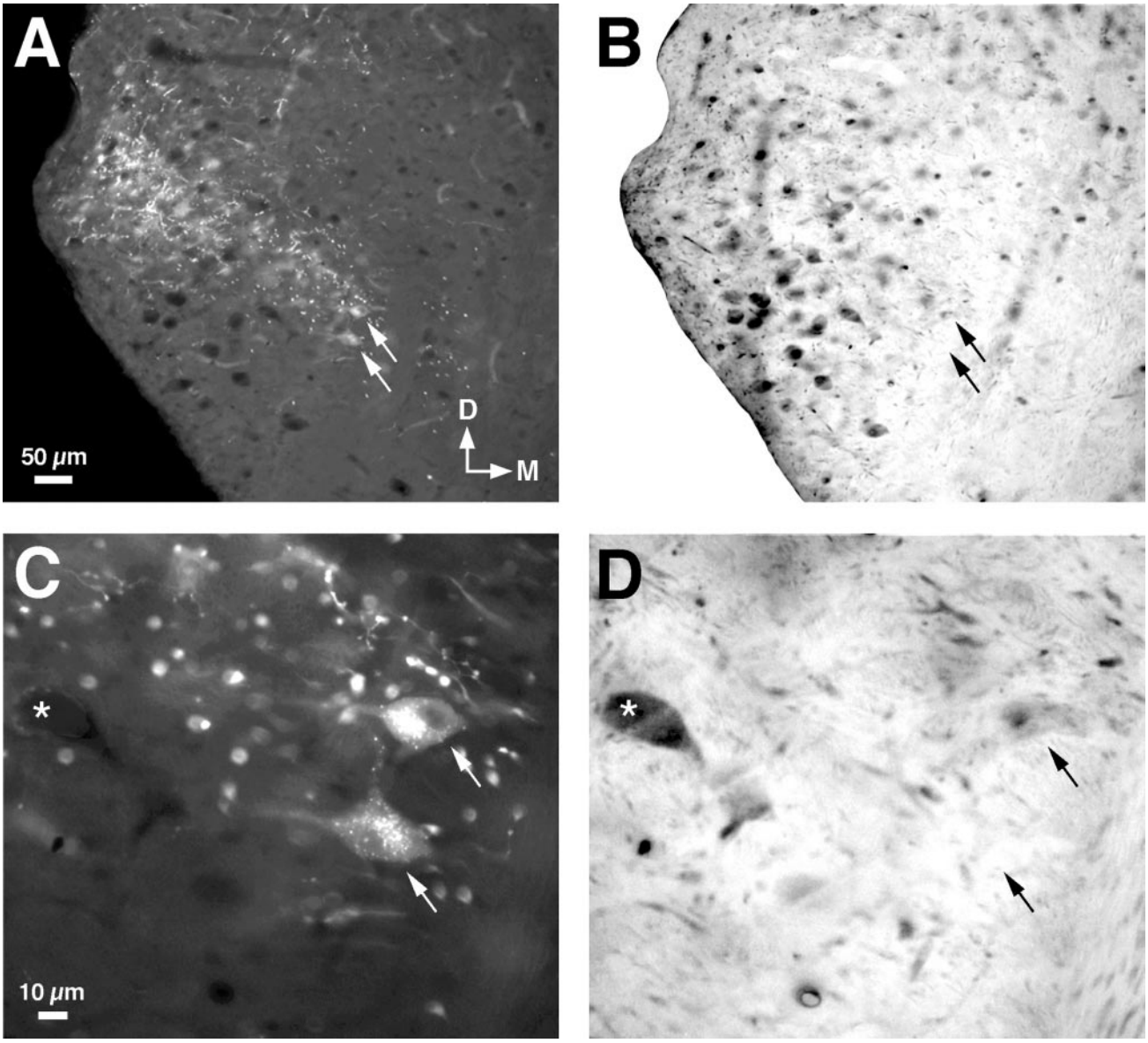

Fig. 8. Retrogradely labeled planar neurons can be lightly stained when processed with antibodies directed against glycine. **A:** Fluorescent micrograph of a coronal section through a retrogradely labeled stripe in the anteroventral cochlear nucleus (AVCN). Two planar neurons within the stripe are indicated by arrows. **B:** Brightfield photograph of glycine immunostaining in the same field of view and same focal plane as in A. Light glycine immunoreactivity is observed in one planar neuron and no reactivity is observed in the other. The retrogradely labeled (**C**) and glycine-processed (**D**) planar neurons are shown at higher magnification, illustrating the slight variability in immunostaining. Asterisks indicate a glycine-positive neuron (D) whose silhouette can be seen in the fluorescent micrograph (C) following immunohistochemical processing. Scale bars in A and C apply to respective horizontal rows. D, dorsal; M, medial.

the DCN, exhibit separate immunoreactive properties with respect to the glycine antibody. Planar neurons exhibit light glycine immunostaining, similar to that observed in pyramidal cells in the DCN. Because pyramidal neurons exert excitatory influences at their target projection sites (Semple and Aitkin, 1980), the low levels of glycine immunoreactivity in these neurons probably reflect metabolic pools of the amino acid (Osen et al., 1990). In contrast, radiate neurons are darkly immunostained for glycine, and the intensity of their immunoreactivity is similar to that of DCN cartwheel cells and MNTB principal neurons. Cartwheel cells and MNTB principal neurons are known to be glycinergic (Moore and Caspary, 1983; Wenthold et al., 1987; Bledsoe et al., 1990; Davis and Young, 1997) and so the glycine enrichment of radiate neurons is consistent with the idea that they use glycine as their neurotransmitter and provide an inhibitory projection from the VCN to the DCN.

Our interpretation of the pattern of retrograde labeling in the VCN is that planar and radiate neurons form terminal arborizations within the DCN injection site. Although the injection sites were near the dorsal and intermediate acoustic striae, neurons that do not terminate within the injection site but that are known to send

their axons through the dorsal output tracts were never labeled (octopus cells; pyramidal and giant cells outside the injection site). Thus, we are confident that these tracts were not involved in the injection site and that labeling was not a result of uptake by "fibers-of-passage".

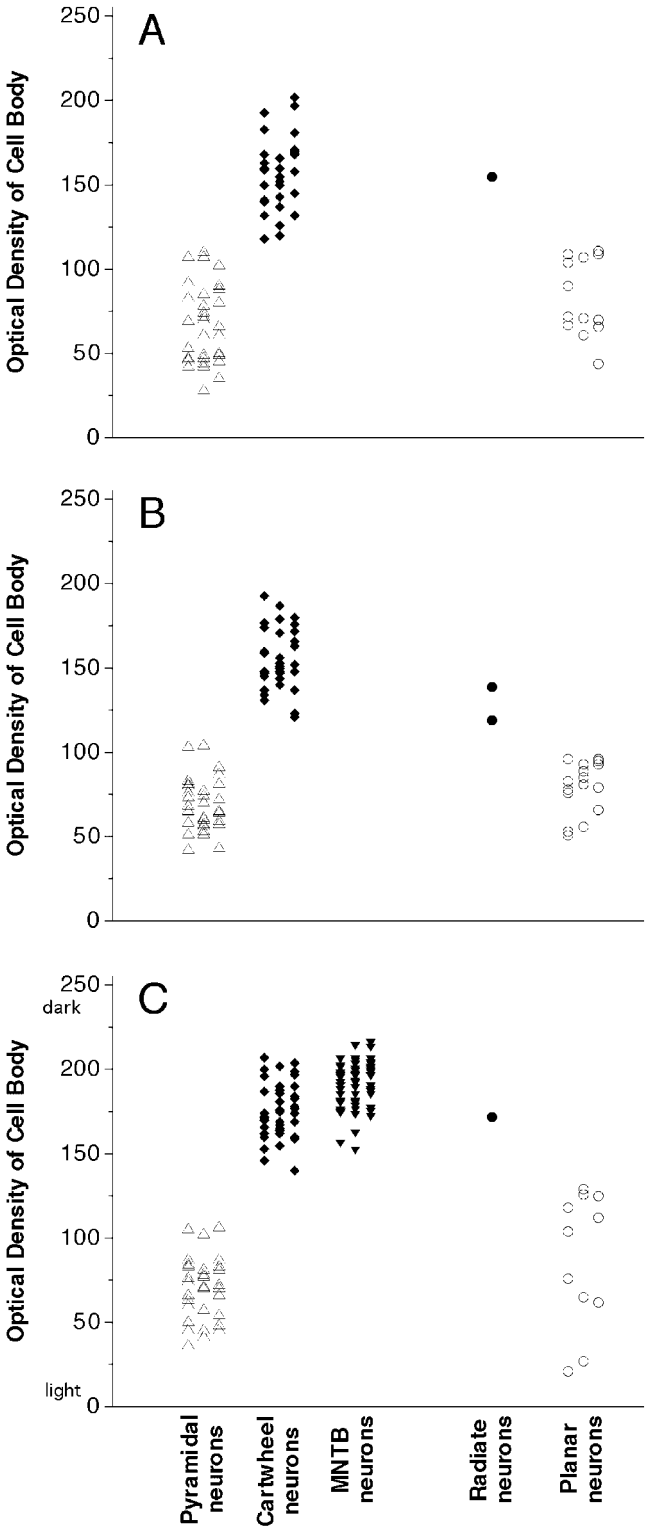

Many different types of neurons were immunostained with the glycine immunocytochemical protocol used in this study, although at very different levels of intensity. This pattern of glycine immunoreactivity has been observed previously using a variety of glycine antibodies, histochemical protocols, and species (Wenthold et al., 1987; Osen et al., 1990; Kolston et al., 1992; Moore et al., 1996). The modest immunostaining of neurons known to be excitatory is attributable to glycine being involved in cellular functions common to all neurons (e.g., protein synthesis), not to its role in neurotransmission. The presence or absence of glycine immunoreactivity in a particular cell class cannot by itself be used to determine function, but the relative intensity of immunoreactivity may be used to distinguish glycinergic and nonglycinergic neurons (Osen et al., 1990). We used the same strategy in our study where DCN cartwheel cells and MNTB principal neurons (glycinergic) were far more darkly stained than DCN pyramidal cells (nonglycinergic). The light immunostaining of planar neurons, comparable to DCN pyramidal and giant cells, makes it unlikely that they use glycine as their neurotransmitter. In contrast, the dark immunostaining of radiate neurons, comparable to DCN cartwheel cells and MNTB principal neurons, implies that they do use glycine as a neurotransmitter and that they inhibit their postsynaptic targets.

Radiate and commissural neurons

Striking morphological similarities have been noted with respect to radiate and commissural neurons (Schofield and Cant, 1996; Doucet and Ryugo, 1997). Commissural neurons are a population of large VCN multipolar neurons that project to the contralateral cochlear nucleus (Cant and Gaston, 1982; Schofield and Cant, 1996). Like radiate neurons, commissural neurons exhibit intense glycine immunoreactivity (Wenthold, 1987). The shared morphological and neurochemical characteristics of radiate and commissural neurons required verification that the retrograde labeling observed in the VCN was not contaminated by labeling "fibers-of-passage." The reason for this concern is that our injection sites were near the dorsal output tracts that run just ventral to the DCN, and the axons of VCN commissural neurons are thought to travel out of the nucleus via these pathways (Cant and Gaston, 1982; Osen, et al., 1990). However, our injection sites did not infringe upon these output tracts.

One hypothesis that could account for the shared morphological and neurochemical features of radiate and commissural neurons is that these two populations are in fact the same neurons. A population of VCN multipolar cells inner-

Fig. 9. **A–C:** Optical density measurements obtained from neurons processed by antibodies directed against glycine. Optical density is the average gray scale value of pixels located inside the cell body, and represents a measure of the intensity of the immunoreactivity of a particular neuron. A density value of zero indicates white (no label) and a value of 255 indicates black (intense label). In these three panels, the optical density of planar and radiate neurons from three experiments is compared with "unlabeled" dorsal cochlear nucleus (DCN) pyramidal cells and "labeled" DCN cartwheel cells and medial nucleus of the trapezoid body (MNTB) principal neurons. In each experiment, at least thirty-five neurons of each type were used to form the distribution of cartwheel cells, pyramidal cells, and MNTB neurons. Note that in each experiment, the optical density of radiate cells overlaps with that of cartwheel and MNTB neurons (glycinergic neurons), whereas the optical density of planar neurons resembles that of DCN pyramidal cells (nonglycinergic neurons).

vating both the DCN and the contralateral cochlear nucleus may represent a general mammalian characteristic. In our previous study, we noted that radiate neurons appear to correspond to D-stellate neurons in mice (Oertel et al., 1990) and to onset-chopper units in cats (Smith and Rhode, 1989). D-stellate cells and onset-chopper units are large VCN multipolar neurons that innervate the DCN, but their targets outside the cochlear nucleus are unknown. Resembling commissural neurons, they project their main axons out of the cochlear nucleus via the dorsal output tracts. Onset-chopper units are probably inhibitory (Smith and Rhode, 1989), while both physiological and pharmocological evidence suggests that D-stellate neurons are glycinergic (Ferragamo et al., 1998). However, prior to this study, the contralateral cochlear nucleus was the only known target of the large VCN multipolar neurons enriched in glycine (Wenthold, 1987). At present, it appears that one target of radiate neurons (and also D-stellate cells and onset-chopper units) outside the cochlear nucleus is the contralateral cochlear nucleus.

Functional considerations

The functional anatomy of planar and radiate neurons along with the topography of their projections to the DCN is summarized in schematic form (Fig. 10). Planar neurons, with their restricted dendritic domains, are probably narrowly tuned and send a tonotopic projection to the DCN. They are presumably excitatory because their neurotransmitter is unlikely to be glycine (this study) or GABA (Mugnaini, 1985; Wenthold et al., 1986; Adams and Mugnaini, 1987; Osen et al., 1990; Kolston et al., 1992). Cell types analogous to planar neurons in cats (sustained-chopper units; Smith and Rhode, 1989) and mice (T-stellate neurons; Oertel et al., 1990) also appear to be excitatory. Sustained-chopper units project to the DCN and their terminal swellings contain round vesicles (Smith and Rhode, 1989), a shape usually associated with an excitatory neurotransmitter (Uchizono, 1965). In slice preparations of the mouse cochlear nucleus, when small quantities of glutamate were used to excite VCN neurons, short-latency excitatory postsynaptic potentials (EPSPs) were recorded in giant, pyramidal, and vertical cells of the DCN (Zhang and Oertel, 1993a,b, 1994). These EPSPs could be evoked at several VCN sites that collectively formed a narrow stripe resembling an isofrequency sheet. This pattern implicated T-stellate cells as the source of the EPSPs. The apparently narrowly tuned, tonotopic, and excitatory projection from the VCN to the DCN seems curious because this projection appears to reiterate the input from auditory nerve fibers. One difference is that sustained choppers encode stimulus intensity much more precisely than do auditory nerve fibers (Young et al., 1988; Shofner and Dye, 1989). Perhaps this more accurate intensity information is required by the neural circuits in the DCN in order to produce the exquisite sensitivity of DCN projection neurons to spectral patterns (Nelken and Young, 1994).

Radiate neurons in the VCN appear to provide a source of glycinergic inhibition to their postsynaptic targets in the DCN. An inhibitory projection from the VCN to the DCN has been suggested by a number of prior studies. For example, in an experiment where the cochlear nerve was sectioned and allowed to degenerate, DCN neurons were inhibited when electrical shocks were applied to the VCN (Evans and Nelson, 1973b). Following lidocaine (a sodium channel blocker) injections into the VCN, the inhibition of type IV units in the DCN is weakened (Shofner and Young, 1987). Multipolar neurons similar to radiate neurons in the mouse (D-stellate) and cat (onset-chopper) that project to the DCN appear to be inhibitory (Smith and Rhode, 1989, Oertel et al., 1990; Ferragamo et al., 1998). We have shown that glycinergic radiate neurons distributed over a broad frequency region in the VCN target a narrow frequency region in the DCN. This topography for the inhibitory input is supported by experiments in the mouse cochlear nucleus. When glutamate was used to excite VCN neurons in the slice preparation, both short-latency EPSPs and inhibitory postsynaptic potentials (IPSPs) were recorded from giant and pyramidal cells in the DCN (Zhang and Oertel, 1993a, 1994). The VCN sites of glutamate application that evoked EPSPs tended to form a stripe resembling an isofrequency sheet, whereas the IPSPs in some cells were elicited from sites almost anywhere along the dorsal-ventral (i.e., frequency) axis of the VCN (Zhang and Oertel, 1993a, 1994). This result is what one would predict based on the functional sign of radiate neurons, their dendritic orientation, and the topography of their projections to the DCN (Fig. 10).

We suggested in a previous study that radiate neurons may function as a broadly tuned source of inhibition to their target neurons in the DCN (Doucet and Ryugo, 1997). In the present study, we strengthened this hypothesis by demonstrating that radiate neurons are enriched in glycine. Broadband inhibition in the DCN has been suggested as a possible role for D-stellate cells in mice (Oertel et al., 1990) and onset-chopper units in cats and guinea pigs (Nelken and Young, 1994; Winter and Palmer, 1995). The most straightforward example of broadband inhibition in the DCN is the type II unit, excited by pure tones near its characteristic frequency (CF) but virtually unresponsive to broadband noise (Evans and Nelson, 1973a; Young and Brownell, 1976). A broadly tuned inhibitory input (called the "wideband inhibitor") has also been hypothesized to target type IV units in order to explain their weak responses (relative to auditory nerve fibers) to broadband noise (Nelken and Young, 1994). Although most studies of DCN physiology have been performed in the cat, Type II and Type IV units are also found in guinea pigs (Stabler et al., 1996) and gerbils (Davis et al., 1996), suggesting that common neural mechanisms underlie their responses to sound. The shared features of D-stellate cells, onset-choppers, and radiate neurons support the idea that the DCN receives a glycinergic projection from radiate neurons of the VCN, and that these neurons represent the structural correlate of onset-chopper units, which provide the physiologically defined wideband inhibition in the DCN.

The "off-frequency" or wideband inhibition schematized in Figure 10 may play a key role in the functional properties of the DCN. The DCN projection neurons (type IV units) are sensitive to narrowband spectral features such as peaks or valleys of energy in a broadband stimulus that contains energy at their CF (Spirou and Young, 1991; Nelken and Young, 1994). This property suggests that DCN projection neurons might be "spectral contrast detectors," thereby identifying to higher auditory centers those frequency regions that contain features important for sound identification or localization (Nelken and Young, 1994). Spectral contrast is detected by comparing the amount of stimulus energy lying in a narrow frequency

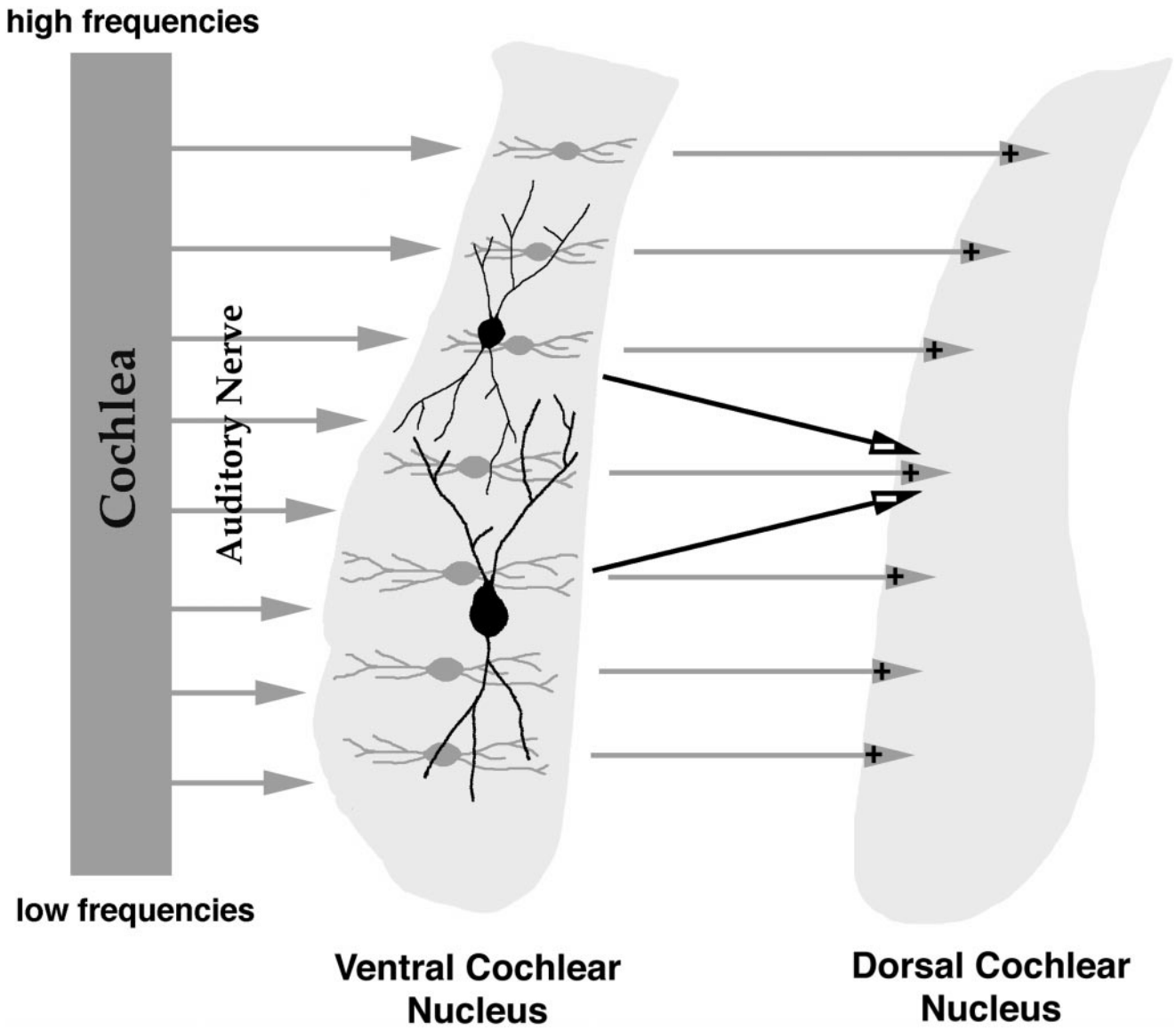

Fig. 10. Schematic diagram summarizing the morphology, neurochemistry, innervation, and action in the dorsal cochlear nucleus (DCN) of planar and radiate neurons. On the left side of the figure, the tonotopic innervation of the ventral cochlear nucleus (VCN) by auditory nerve fibers is depicted. The tonotopic innervation of the DCN by the auditory nerve is not shown in order to keep the illustration simple, and the DCN has been rotated so that its frequency axis is parallel to that of the VCN. Planar neurons (gray) have dendrites that are oriented parallel to the isofrequency sheets formed by auditory nerve fibers and project tonotopically to the DCN. Radiate neurons (black) have dendrites that are oriented orthogonal to VCN isofrequency sheets. The innervation by both planar and radiate neurons of only one DCN isofrequency sheet is schematized, but we expect that this general pattern is maintained for all regions of the DCN. Each DCN isofrequency sheet is hypothesized to receive excitatory projections from similarly tuned planar neurons, and inhibitory projections from surrounding frequency regions through the action of radiate neurons. This innervation pattern suggests a circuit designed to enhance the responses of DCN neurons to spectral contrast.

band to the average level of the stimulus energy in surrounding frequency regions. Information regarding the average level of the stimulus over a broad spectral region could be provided by radiate neurons. Because radiate neurons are inhibitory, they might serve to desensitize their DCN target neurons to flat spectra such as broadband noise, thereby helping to conserve the dynamic ranges of DCN neurons and facilitating their response to peaks and notches of spectral energy near their CFs. This scheme represents a simplified version of DCN circuitry, but the properties of radiate neurons and their innervation of the DCN support the idea that this nucleus is designed to detect spectral contrast.

ACKNOWLEDGMENTS

We thank Brian Rosenbaum and Hugh Cahill for technical assistance, Dr. Charles J. Limb for critical readings of the manuscript, and Dr. Michael Zidanic and Dr. Eric Young for helpful discussions of the data. Portions of these

data were presented in preliminary fashion at the 20th Midwinter Meeting of the Association for Research in Otolaryngology, St. Petersburg Beach, FL, February 2–6, 1997.

LITERATURE CITED

Adams JC. 1983. Multipolar cells in the ventral cochlear nucleus project to the dorsal cochlear nucleus and the inferior colliculus. Neurosci Lett 37:205–208.

Adams JC, Mugnaini E. 1987. Patterns of glutamate decarboxylase immunostaining in the feline cochlear nuclear complex studied with silver enhancement and electron microscopy. J Comp Neurol 262:375–401.

Albanese A, Bentivoglio M. 1982. Retrograde fluorescent neuronal tracing combined with acetylcholinesterase histochemistry. J Neurosci Methods 6:121–127.

Aoki E, Semba R, Keino H, Kato K, Kashiwamata S. 1988. Glycine-like immunoreactivity in the rat auditory pathway. Brain Res 442:63–71.

Berrebi AS, Mugnaini E. 1991. Distribution and targets of the cartwheel cell axon in the dorsal cochlear nucleus of the guinea pig. Anat Embryol 183:427–454.

Bledsoe SC Jr, Snead CR, Helfert RH, Prasad V, Wenthold RJ, Altschuler RA. 1990. Immunocytochemical and lesion studies support the hypothesis that the projection from the medial nucleus of the trapezoid body to the lateral superior olive is glycinergic. Brain Res 517: 189–194.

Bourk TR, Mielcarz JP, Norris BE. 1981. Tonotopic organization of the anteroventral cochlear nucleus of the cat. Hear Res 4:215–241.

Cant NB, Gaston KC. 1982. Pathways connecting the right and left cochlear nuclei. J Comp Neurol 212:313–326.

Davis KA, Young ED. 1997. Granule cell activation of complex-spiking neurons in dorsal cochlear nucleus. J Neurosci 17:6798–6806.

Davis KA, Jiang D, Benson TE, Voigt HF. 1996. Response properties of units in the dorsal cochlear nucleus of unanesthetized decerebrate gerbils. J Neurophysiol 75:1411–1431.

Doucet JR, Ryugo DK. 1997. Projections from the ventral cochlear nucleus to the dorsal cochlear nucleus in rats. J Comp Neurol 385:245–264.

Eckenstein F, Sofroniew MV. 1983. Identification of central cholinergic neurons containing both choline acetyltransferase and acetylcholinesterase and of central neurons containing only acetylcholinesterase. J Neurosci 3:2286–2291.

Evans EF, Nelson PG. 1973a. The responses of single neurones in the cochlear nucleus of the cat as a function of their location and anesthetic state. Exp Brain Res 17:402–427.

Evans EF, Nelson PG. 1973b. On the functional relationship between the dorsal and ventral divisions of the cochlear nucleus of the cat. Exp Brain Res 17:428–442.

Fekete DM, Rouiller EM, Liberman MC, Ryugo DK. 1984. The central projections of intracellularly labeled auditory nerve fibers in cats. J Comp Neurol 229:432–450.

Ferragamo MJ, Golding NL, Oertel D. 1998. Synaptic inputs to stellate cells in the ventral cochlear nucleus. J Neurophysiol 79:51–63.

Gates TS, Weedman DL, Pongstaporn T, Ryugo DK. 1996. Immunocytochemical localization of glycine in a subset of cartwheel cells of the dorsal cochlear nucleus in rats. Hear Res 96:157–166.

Helfert RH, Bonneau JM, Wenthold RJ, Altschuler RA. 1989. GABA and glycine immunoreactivity in the guinea pig superior olivary complex. Brain Res 501:269–286.

Jiang D, Palmer AR, Winter IM. 1996. The frequency extent of two-tone facilitation in onset units in the ventral cochlear nucleus. J Neurophysiol 75:380–395.

Kalloniatis M, Fletcher EL. 1993. Immunocytochemical localization of the amino acid neurotransmitters in the chicken retina. J Comp Neurol 336:174–193.

Kaltenbach JA, Lazor J. 1991. Tonotopic maps obtained from the surface of the dorsal cochlear nucleus of the hamster and rat. Hear Res 51: 149–160.

Kolston J, Osen KK, Hackney CM, Ottersen OP, Storm-Mathisen J. 1992. An atlas of glycine- and GABA-like immunoreactivity and colocalization in the cochlear nuclear complex of the guinea pig. Anat Embryol 186:443–465.

Liberman MC. 1991. Central projections of auditory-nerve fibers of differing spontaneous rate. I. Anteroventral cochlear nucleus. J Comp Neurol 313:240–258.

Liberman MC. 1993. Central projections of auditory-nerve fibers of differing spontaneous rate. II. Posteroventral and dorsal cochlear nuclei. J Comp Neurol 327:17–36.

Lorente de Nó R. 1981. The primary acoustic nuclei. New York: Raven Press.

Manis PB, Spirou GA, Wright DD, Paydar S, Ryugo DK. 1994. Physiology and morphology of complex spiking neurons in the guinea pig dorsal cochlear nucleus. J Comp Neurol 348:261–276.

Moore MJ, Caspary DM. 1983. Strychnine blocks binaural inhibition in lateral superior olivary neurons. J Neurosci 3:237–242.

Moore JK, Osen KK, Storm-Mathisen J, Ottersen OP. 1996. GABA and glycine in the baboon cochlear nuclei: An immunocytochemical colocalization study with reference to interspecies differences in inhibitory systems. J Comp Neurol 369:497–519.

Mugnaini E. 1985. GABA neurons in the superficial layers of rat dorsal cochlear nucleus: light and electron microscopic immunocytochemistry. J Comp Neurol 235:537–570.

Nelken I, Young ED. 1994. Two separate inhibitory mechanisms shape the responses of dorsal cochlear nucleus type IV units to narrowband and wideband stimuli. J Neurophysiol 71:2446–2462.

Oertel D, Wu SH. 1989. Morphology and physiology of cells in slice preparations of the dorsal cochlear nucleus of mice. J Comp Neurol 283:228–247.

Oertel D, Wu SH, Garb MW, Dizack C. 1990. Morphology and physiology of cells in slice preparations of the posteroventral cochlear nucleus of mice. J Comp Neurol 295:136–154.

Oliver DL. 1984. Quantitative analyses of axonal endings in the central nucleus of the inferior colliculus and distribution of 3H-labeling after injections in the dorsal cochlear nucleus. J Comp Neurol 237:343–359.

Osen KK, Ottersen OP, Storm-Mathisen J. 1990. Colocalization of glycine-like and GABA-like immunoreactivities: A semiquantitative study of individual neurons in the dorsal cochlear nucleus of cat. In: Ottersen OP, Storm-Mathisen J, editors. Glycine neurotransmission. New York: John Wiley & Sons. p 417–451.

Ottersen OP, Storm-Mathisen J, Laake JH. 1990. Cellular and subcellular localization of glycine studied by quantitative election microscopic immunocytochemistry. In: Ottersen OP, Storm-Mathisen J, editors. Glycine neurotransmission. New York: John Wiley & Sons. p 303–328.

Palmer AR, Jiang D, Marshall DH. 1996. Responses of ventral cochlear nucleus onset and chopper units as a function of signal bandwidth. J Neurophysiol 75:780–794.

Peyret D, Campistron G, Geffard M, Aran JM. 1987. Glycine immunoreactivity in the brainstem auditory and vestibular nuclei of the guinea pig. Acta Otolaryngol 104:71–76.

Rhode WS, Smith PH. 1986. Encoding timing and intensity in the ventral cochlear nucleus of the cat. J Neurophysiol 56:261–286.

Rose JE, Galambos R, Hughes J. 1960. Organization of frequency sensitive neurons in the cochlear nuclear complex of the cat. In: Rasmussen GC, Windle WF, editors. Neuronal mechanisms of the auditory and vestibular systems. Springfield, IL: Thomas. p 116–136.

Ryugo DK, May SK. 1993. The projections of intracellularly labeled auditory nerve fibers to the dorsal cochlear nucleus of cats. J Comp Neurol 329:20–35.

Ryugo DK, Willard FH, Fekete DM. 1981. Differential afferent projections to the inferior colliculus from the cochlear nucleus in the albino mouse. Brain Res 210:342–349.

Saint Marie R L, Benson CG, Ostapoff EM, Morest DK. 1991. Glycine immunoreactive projections from the dorsal to the anteroventral cochlear nucleus. Hear Res 51:11–28.

Schofield BR, Cant NB. 1996. Origins and targets of commissural connections between the cochlear nuclei in guinea pigs. J Comp Neurol 375:128–146.

Semple MN, Aitkin LM. 1980. Physiology of pathway from dorsal cochlear nucleus to inferior colliculus revealed by electrical and auditory stimulation. Exp Brain Res 41:19–28.

Shofner WP, Dye RH. JR. 1989. Statistical and receiver operating characteristic analysis of empirical spike-count distributions: quantifying the ability of cochlear nucleus units to signal intensity changes. J Acoust Soc Am 86:2172–2184.

Shofner WP, Young ED. 1987. Inhibitory connections between AVCN and DCN: evidence from lidocaine injection in AVCN. Hear Res 29:45–53.

Smith PH, Rhode WS. 1989. Structural and functional properties distinguish two types of multipolar cells in the ventral cochlear nucleus. J Comp Neurol 282:595–616.

Snyder RL, Leake PA. 1988. Intrinsic connections within and between cochlear nucleus subdivisions in cat. J Comp Neurol 278:209–225.

Spirou GA, Berrebi AS. 1997. Glycine immunoreactivity in the lateral nucleus of the trapezoid body of the cat. J Comp Neurol 383:473–488.

Spirou GA, Young ED. 1991. Organization of dorsal cochlear nucleus type IV unit response maps and their relationship to activation by bandlimited noise. J Neurophysiol 66:1750–1768.

Spirou GA, May BJ, Wright DD, Ryugo DK. 1993. Frequency organization of the dorsal cochlear nucleus in cats. J Comp Neurol 329:36–52.

Stabler SE, Palmer AR, Winter IM. 1996. Temporal and mean rate discharge patterns of single units in the dorsal cochlear nucleus of the anesthetized guinea pig. J Neurophysiol 76:1667–1668.

Uchizono K. 1965. Characteristics of excitatory and inhibitory synapses in the central nervous systems of the cat. Nature 207:642–643.

Voigt HF, Young ED. 1980. Evidence of inhibitory interactions between neurons in dorsal cochlear nucleus. J Neurophysiol 44:76–96.

Wenthold RJ. 1987. Evidence for a glycinergic pathway connecting the two cochlear nuclei: an immunocytochemical and retrograde transport study. Brain Res 415:183–187.

Wenthold RJ, Zempel JM, Parakkal MH, Reeks KA. 1986. Immunocytochemical localization of GABA in the cochlear nucleus of the guinea pig. Brain Res 380:7–18.

Wenthold RJ, Huie D, Altschuler RA, Reeks KA. 1987. Glycine immunoreactivity localized in the cochlear nucleus and superior olivary complex. Neuroscience 22:897–912.

Wickesberg RE, Oertel D. 1988. Tonotopic projection from the dorsal to the anteroventral cochlear nucleus of mice. J Comp Neurol 268:389–399.

Wickesberg RE, Whitlon D, Oertel D. 1991. Tuberculoventral neurons project to the multipolar cell area but not to the octopus cell area of the posteroventral cochlear nucleus. J Comp Neurol 313:457–468.

Winter IM, Palmer AR. 1995. Level dependence of cochlear nucleus onset responses and facilitation by second tones or broadband noise. J Neurophysiol 73:141–159.

Young ED, Brownell WE. 1976. Responses to tones and noise of single cells in dorsal cochlear nucleus of unanesthetized cats. J Neurophysiol 39:282–300.

Young ED, Shofner WP, White JA, Robert J-M, Voigt HF. 1988. Response properties of cochlear nucleus neurons in relationship to physiological mechanisms. In: Edelman GM, Gall WE, Cowan WM, editors. Auditory function: neurobiological bases of hearing. New York: John Wiley & Sons. p 277–312.

Zhang S, Oertel D. 1993a. Giant cells of the dorsal cochlear nucleus of mice: intracellular recordings in slices. J Neurophysiol 69:1398–1408.

Zhang S, Oertel D. 1993b. Tuberculoventral cells of the dorsal cochlear nucleus of mice: intracellular recordings in slices. J Neurophysiol 69:1409–1421.

Zhang S, Oertel D. 1994. Neuronal circuits associated with the output of the dorsal cochlear nucleus through fusiform cells. J Neurophysiol 71: 914–930.